Calibration of the Extragalactic Distance Scale: Tip of the Red Giant Branch Distance to NGC 337'9 (M105) in the Leo 1 Group

DRAFT 12/03/95

Shoko Sakai

Jet Propulsion Laboratory, California Institute of Technology

MS 100-22, *Pasadena, CA 91125*

Barry F. Madore

NASA /IPAC Extragalactic Database, Infrared Processing and Analysis Center

California Institute of Technology, MS 100-22, Pasadena, CA 91125

Wendy L. Freedman

The Observatories, Carnegie Institution of Washington

813 Santa Barbara Street, Pasadena, CA 91101

and

Tod Lauer

National Optical Astronomy Observatory

P. O. Box 26732 Tucson, AZ 85726

Running Headline: *TRGB Distance to NGC 3379*

Received: _____; *Accepted:* _____

Abstract

We report the unambiguous detection of individually resolved stars in the elliptical galaxy NGC *3379*, a luminous member of the Leo 1 Group. The bright end of the stellar luminosity function has a logarit hmic slope that is consistent with these stars being Population II red giants. An abrupt discontinuity in the apparent luminosity function at I = 26.294 0.10 mag is identified with the tip of the first- ascent red giant branch (TRGB). Adopting M_I (TRGB) = -4.0 ± 0.1 mag gives a distance modulus of 30.294 0.14 mag corresponding to a linear distance to NGC 3379 of 1 I.4 ± ().8 Mpc. The TRGB distance compares very wc]] with the Cepheid distance of 1].6 ± 0.8 Mpc *(30.32* ± 0.16 mag) to another group member M96 (= NGC 3368). This constitutes the first direct determination of a distance to a giant elliptical galaxy which can be used in turn to calibrate the zero points of three secondary distance determination methods: surface brightness fluctuations, planetary nel ula luminosity functions, and the D_n-σ m eth od. We apply several different approa ches to m easure the Hubble constant : (]) a simple Virgocentric infall model , (2) stepping OUt from] .eo] to th C Coma C] uster via Virgo using three different secondary distance indicators and their new zero points, and (3) stepping directly to Coma using the D_n - σ relation. A l l techniques give a consistent value Of Hubble constant Of H_o = 70 ± 11 km s^{-1} Mpc^{-1}.

Subject ***headings:*** galaxies: individual galaxies: elliptical galaxies - galaxies: distances

1 introduction

There are several paths to a far- field estimation of the Hubble constant. But these paths are often complicated by a series Of arguable, but necessary, assumptions, where external checks and comparisons can be difficult, or impossible due to largely non-overlapping data sets. On the other hand, various measures of the IIcaI-field distance scale (largely made within the Local Group) arc in excellent agreement, having benefited from numerous recent intercomparisons of distances to the nearest galaxies. Using both Population I and Population 11 distance determination methods the local distance scale appears to have converged at the :I- 10-- 20%0 level (see Freedman & M adore 1993, *1* 995; Hutterer, Sasselov & Schechter] 995). Cepheids have long been the cornerstone of the Population] route; and RR Lyraes have more recently provided the best Population 11 counterpoint. But RR Lyrae stars are intrinsically fainter than classical Cepheids, making their application to galaxies significantly beyond the Local Group unlikely in the foreseeable future.

1 lowever, there are Population 11 stars brighter than the horizontal branch variables. Indeed, the brightest red giant branch (RGB) stars, identified by their first appearance as a discontinuity in the bright end of the luminosity function of the first-ascent (Population 11) RGB population has also been shown to be extremely stable in luminosity, while being some 40 times brighter than the RR Lyrae stars. In the *I*- band, this TRGB ("tip-of-the-red-giant-branch") method as a distance indicator is only slightly sensitive to metallicity (over a wide range of ages and metallicities applicable to old galaxy populations (see Lee, Freedman *and* Madore 1 993).

The first- ascent red giant branch marks the core helium flash of low- mass stars which evolved along the red giant bran ch up to the tip, at which point the luminosity function abruptly terminates. In *I* – band, the TRGI3 resolves at $M_I \sim$ - 4 mag. This discontinuity has been shown to be an excellent distance indicator, since the bolometric luminosity of the

TR GB varies only by ~0. 1 mag for ages ranging from 2 up to 15 Gyr (cf. Iben & Renzini I 983), and metallicities in the range represented by Galactic globular clusters (- 2.1 $\leq$ [Fe/H] $\leq$ --().7). The red giant branch luminosity function also has another characteristic feature that can be used to corroborate the detection of the TRGB; it has a logarithmic slope of 0 . 6 dex/mag (*e.g.,* Ortiz 1990; Sakai, Madore & Freedman 1996). Theoretically predicted and now empirically tested and confirmed, the TRGB is an outstanding distance indicator. Furthermore, it is applicable to all morphological types of galaxies. Since they represent the evolved component of older generations of stars in galaxies, TRGB stars are naturally found in both elliptical galaxies and spiral halos, as w c]] as in the "Baade's red sheet" populations of irregular galaxies.

It is important to note the significance of the TRGB method as a pure application of a Population 11 distance indicator. Several secondary distance indicators which enable us to investigate the density and velocity fields at cosmologically significant distances, including surface brightness flue.tuatio]ls, planetary nebula luminosity functions and the D_n - σ relation, all strongly depend on the old E/S0 galaxy populations. Since Cepheid variables are not found in these systems, and because of the lack of elliptical systems within or even near to the Local Group, the absolute calibration of such Pop II methods has either had to rely 011 the distance to a single galaxy (*e.g.* the bulge of M31), or Cepheid (Pop I) distances to spiral galaxies in the same group or cluster. The TRGB method instead can provide a *direct* distance to an elliptical galaxy. *And in this* payer, *we use Population 11 distance indicators 10 estimate the value of* H_0 *completely independently of Cepheid 1'1, relation.*

Using computer simulations, Madore & Freedman (] 995) have investigated the distance out to which the TRGB method of distance determination is applicable. They conclude that from the ground under optimal conditions of seeing, distances of 2 - 3 Mpc are possible and that a factor of ten further can be achieved with the HST.] Dist ances slightly in excess

of 1 Mpc have already been measured from the ground using the TRGB under moderate (1 .3 arcsec) seeing conditions (*e.g.*, Sakai, Madore & Freedman 1996). We report here the first space based application of this method to an elliptic.a] galaxy, NGC 3379 in the Leo 1 Group. This constitutes the most distant application of the TRGB method to date, and its first application to a giant elliptical galaxy.

Using data obtained with the Hubble Space Telescope (HS'J'), we present in the next section observations and data reduction procedures, followed by the application of the TRGB method to the I-band luminosity function for stars in the halo of NGC 3379. We conclude by presenting some implications for the value of Hubble constant.

2 Observations and **Data Reduction**

The observations of NGC 3379 were made in May 1994 using the Wide Field and Planetary Camera 2 (WFPC2). A sequence of 32 exposures of 900 sec each were obtained using the F814W filter, amounting to a total integration time of 8 hours. The target field was centered at $\alpha_{2000.0} = 10^h47^m49^s.4$ and $\delta_{2000.0} = 12^d34^m57^s.1$ which is 6 arcmin due west of the nucleus of NGC 3379 (see Plate 1). [TOD; YOU WILL WAN'] ' TO FILL IN THIS PARAGRAPH AND DESCRIBE THE MOTIVATION FOR CHOOSING THE FIELD THAT YOU DID.]

The data. qualify files, provided by the HST data- processing pipeline, and vignetting masks were used to mark bad pixels on the images. To dca] with the problem of the geometric distortion of the WFPC2 optics, we used the pixel area map provided by Holtzman to restore the integrity of the flux measurements. Once the galaxy images were processed through these steps, all 32 frames were combined using an IRAF routine "imcombine" with the 3- σ clipping option to remove obvious cosmic rays.

The stellar photometry was then carried out using the packages DAOPHOT and ALL-

STAR (Stetson 1987). These programs use automatic star finding algorithms and then measure stellar magnitudes by fitting a])oi])t-spread function (PSF), constructed from other uncrowded images (Stetson 1 994). The 1"814W- filter PSF magnitudes were transformed to Cousins I and corrected to 1- sec exposure time, following the calibration prescriptions given by Stetson (1 995). The transformation equation is:

$$I = m_{DAOPHOT} + 2.5 \log t - C, \quad (1)$$

where C equals --1.872 mag for WF2 and --1.913 mag for WF4. Since we only have I - band observations of N3379, no color information on the stars is available. However, the color term in the calibration is very small, and would amount to approximately 0.04 mag at, most (2% in distance) even for $(V - I)$ colors of 2, the color of a very red giant branch. We note that the integrated color of this galaxy is (V -- I) = 1.2 mag (Tonry *et al.* 1990).

3 The luminosity Function

Using IIAO1'I1O'J', we have found ~13,000 objects on each chip. In order to discriminate Hon-stellar objects, such as background galaxies, we use the χ^2 value which is one of the standard fitting parameters reported by ALLSTAR, giving the goodness of fit of PSF to the object profile itself. Limiting the database to objects with $\chi^2 < 1.6$ (effectively selecting the most likely stellar candidates), we reduced the number of objects down to ~1 .500 per chip. This is rather a conservative selection of objects, We have also checked brightest stars ($I \leq 27.0$ mag) visually on each chip to make sure that they were not contaminated by background galaxits.

Although no color information is available, the form and slope of the observed I - band luminosity function for star-like objects in the NGC 3379 frames present compelling evidence that what we are seeing is indeed the first- ascent red giant branch. The abrupt turn-on of the luminosity function is *prima facia* evidence that we have resolved Population 11 stars. Is

it conceivable that these could be intermediate age asymptotic giant branch (AGB) stars or even a rare population of stars not seen in any quantity in Local Group galaxies? Evidence that *this is not the case* is provided by the additional information available to us about the slope of the luminosity function (faintward of the discontinuity) which is fully consistent with that of a standard reel-giant population. Top panels in Figure 1 show I-band luminosity function for the stellar data found on all chips. We have only included those stars with photometric errors Icss than 0.'20 mag in this analysis, The rapid rise in the numbers of stars at $I \sim$ 26 mag shows unmistakably the TRGB. Following this, there is a shallower but still monotonic rise in the counts with a logarithmic slope of $\sim$0.6 dex/mag up to $I \sim$ 27.5 mag at which point incompleteness due to photon statistics Lakes over and truncates the data. The logarithmic slope of 0.6 is consistent with that for a Population 11 RGB stars in the LMC (Ortiz 1990); ant] also holds for the RGB population in Sextans A (Sakai, Madore & Freedman 1996).

It is noteworthy that brightward of the TRGB in the NGC 3379 halo star population, there is scant evidence for an appreciable AGB population. In the interval two magnitudes brightward of the tip wc find only 70 stars. In a practical sense this feature (or rather the lack thereof) provides for a very clean definition of the tip magnitude, but also puts very hard limits on the contribution of any intermediate-age population.

4 The TRGB Distance

From previous work (see Lee, Freedman & Madore 1993; Madore & Freedman 1995 and references therein), we expect to detect stars achieving the peak luminosity along the first- ascent red giant branch at an absolute I- band magnitude of -4.0 mag. It has been demonstrated empirically, and there is a theoretical basis for expecting that in the specific wavelength range defined by the I- band filter ($\sim$8000 A), the absolute magnitude of the

TRGB is least sensitive to age and metallicity. Residual metallicity effects on the absolute magnitude have been calibrated (Lee, Freedman & Madore 1993), making the I- band magnitude of the TRGB a stable and luminous Population 11 extragalactic distance indicator.

We use both kernel-smoothed linear luminosity distribution and the logarithmic luminosity function to determine the luminosity of the TRGB. When the adopted edge detection filter is applied to a distribution] having a sudden discontinuity on the bright side leading to a constant- slope distribution on the faint side (such as the one sought here), the filter output will Snow a significant positive response at the discontinuity followed by a plateau at the new slope (see Figure 1 in Madore & Freedman 1996). In Sakai, Madore & Freedman (1 996), we introduced a kernel-smoothed luminosity function (but not logarithmic) filtered by a modified Sobel kernel; here, we apply the identical edge detection filter to the logarithmic luminosity distribution as well to determine the magnitude of the TRGB. The logs.rithlnic luminosity function is preferred because of its characteristic slope of 0.6 mag/dex for the RGB population which should be more easily detected by the edge-detection filter. In addition, we apply a weighting scheme to the filtered response function. The edge detection filter essentially measures the slope, and thus it is extremely sensitive to noise; any sudden change in signal is amplified by the filtering scheme. If the luminosity function is expressed by $\Phi(I)$, the response function at I is derived via $E(I) = \log \Phi(I + \sigma) - \log \Phi(I - \sigma)$ where σ is a typical error for stars of magnitude I (see Appendix of Sakai, Madore & Freedman 1996 for details). Each $E(I)$ is weighted by a square root of $\log \Phi(I)$. The weighting scheme was used in order to suppress those statistically- insignificant responses due to noisy data. In the bottom panels of Figure 1, the corresponding response functions from the edge detection filtering are plotted. Inspecting both response functions, we report an unambiguous detection of the TRGB at $I = 26.31 \pm 0.10$ mag. The jump in luminosity function at this magnitude followed by the 0.6 mag/dex slope faintward of the tip in the top right panel helps in further confirming the detection of the red giant branch population. The WF4 field is least contar-

inated by background galaxies and its stellar population is the dominant source of signal in the combined response function.

However, note also that there is a substantial signal at I = 25.9 mag in the logarithmic representation of the data. Could this be the TRGB? This appears unlikely because, as shown below, this peak is not a robust feature. We studied the reliability of each signal by calculating the error in each bin in the response function histogram. If the ith magnitude bin has N_i counts, its Poisson error is simply $\sqrt{N_i}$. For each luminosity function bin, we perturbed its number randomly following a Gaussian distribution]) whose dispersion was set to $\sqrt{N_i}$. For each iteration of randomly displaced luminosity function, we re applied the edge detection filter and measured the response function. An average response histogram of all 500 iterations is plotted in Figure 2. The 1 σ errors for each bin are now shown. It is clear that all the 'signals' below I = 26.0 mag are very likely due to noise, while the TRGB signal remains stable.

Taking into account the Galactic extinction correction along the line of sight to NGC 3379, which amounts to only 0.02 mag (Burstein & Heiles 1978) in the I-band, we adopt I_o = 26.29 mag for the TRGB. It is assumed that the internal reddening in NGC 3379 is negligible as the target field is placed 6 arcmin away from the nucleus, ant] we apply 110 correction here. The TRGB distance modulus is derived via a relation $(m - M)_{TRGB} = I_{TRGB} + BC_I - M_{bol,TRGB}$ where BC_I is the bolometric correction to the I magnitude and $M_{bol,TRGB}$ is the bolometric magnitude of the TRGB stars (Lee *et al.* J 993). BC_I and $M_{bol,TRGB}$ are expressed in terms of metallicity and color: BC_I = 0.881- 0.243$(V - I)_{TRGB}$ and $M_{bol,TRGB}$ = - - 0.19$[Fe/H]$ - 3.81. We must then address what the metallicity of the TRGB halo stars is for NGC 3379. The integrated color of this galaxy is reported to be (V - I) = 1.2 (Tonry *et al.* 1 990); but unfortunately, no published ground-based surface photometry reaches deep enough to determine the surface brightness at the position of the WFPC2 field, 6 arcmin from the nucleus.

1 however by extrapolating the surface photometry data given in Goudfrooji *et al.* (1 994) from r = 2 arcmin to 6 arcmin, we calculate $(B - I)$ = 1.9 ± 0.1 mag. Substituting this value into a relation $[Fe/H] = 2.67(B - I)$ - 5.73 derived from Couture *et al.* (1990), we obtain $[Fe/H]$ = —0.66 ± 0.27. This is only marginally outside the solid calibration of the TRGB. The original calibration of the TRGB method by Lee *et al.* (1 993) applies strictly only to the metallicity range of $-2.2 < [Fe/H] < -0,7$ dex.

Given the understanding that the metallicity of NGC 3379 halo is slightly outside the Galactic globular Cluster metallicity calibration range, we proceed to determine the absolute magnitude of the TRGB for NGC 3379 following Lee *et al.* (1993). WC obtain M_I = --4.04. 0.1 mag. Thus, the TRGB distance modulus for NGC 3379 is 30.29 ± 0.14 mag. This corresponds to a linear distance of 11.4 ± 0.8 Mpc.

5 Comparison with Previously-Published Distances

Within the last 6 years, three new and relatively independent determinations of the distance to NGC 3379 have been published. Ciardullo *et* al, (1 989) have used the planetary nebula luminosity function method to estimate a distance of' 10.0 Mpc (μ_0 = 30.01 mag). Tonry *et al.* (1990) have estimated the distance to NGC 3379 using the surface brightness fluctuation (SBF) method, and they derive 9.4 Mpc (μ_0 = 29.87 mag). Finally, Pahre and Mould (1 995) have also used the SBF method, but applying it in the near infrared K- band rather than in the optical; they obtain a distance of 1 J.1 Mpc (μ_0 = 30.22 mag). The internal agreement of these results and their intercomparison with the TRGB determination presented here are very encouraging. All of these previous determinations rely on a zero point calibration based on the Cepheid determination to M31, (and, in some cases, the companions to M31).

6 The Leo] Group

The Leo 1 Group (= M96 Group = G12 according *to dc* Vaucouleurs 1975), consists of five dominant galaxies: NGC 3368 [M96; SAB(rs)ab], NGC 3351 [M95; SB(r)b], NGC 3384 [S11(s)0], NGC 3377 [E5/6] and NGC 3379 itself [M105; E1]. Two of its spiral members NGC 3368 and NGC 3351 have been the focus of initiatives to measure their distances using Cepheids discovered by HST (Tanvir *et al.* 1995; Graham *et al. 1996)* respectively. At this time, only the data for NGC 3368 (= M96) have been published and they give a true distance modulus of 30.32 ± 0,16 mag which corresponds to a linear distance of 11.6 ± 0.8 Mpc. The remarkable agreement of the Cepheid distance to NGC 3368 and the TRGB distance to NGC 3379 provide additional evidence that the two independent methods are equally accurate and precise. Alternatively, one can take the s])iral/elliptical agreement as strong support for the compact nature of the M96/Leo Group and the physical association of the spiral and elliptical components.

'7 The Hubble Constant

A search of the NED database reveals 15 galaxies within a radius of 5 degrees of M96 and having published radial velocities less than 1,200 km s^{-1}. Their mean velocity in the reference frame of the Local Group (corrected using $V_{LG} = V_{Hel} + 300 \sin l \cos b$) is +842 km s^{-1}. Within the group those 15 galaxies have a velocity dispersion of ±178 km s^{-1}, giving an uncertainty on the mean redshift of ±46 km s^{-1}. Without regard for any additional correction terms for flow velocities at the distance of the M96-Leo Group, the simple velocity-distance ratio is 75 ± 4 km S^{-1} Mpc^{-1}.

'7.1 Virgocentric Infall Model

We now proceed to evaluate the local expansion rate using the most direct (although still overly simplified) approach in which the smooth, unperturbed expansion velocity of NGC 3379 is determined by considering a single perturbation flow model involving only the Virgo duster. Using simple geometry (Figure 3), the Virgocentric infall of the Leo I group can be estimated by scaling the amplitude of the Local Group infall velocity into the Virgo cluster. For instance, Mould *et al.* 1995 quote 331 ± 41 km s^{-1} for the Local Group infall velocity toward Virgo. Wc adopt that value here and take the distance to the Virgo cluster from the Local Group to be 16.1 ± 3.2 Mpc (Ferrarese *et al.* 1996); the large uncertainty reflects the complex geometry of the Virgo cluster. By simple trigonometry, and using linear perturbation theory with an assumption that the density profile of the Virgo duster varies as r^{-2}, wc find that the infall velocity of Leo 1 Group towards Virgo is 707 ± 88 km s^{-1}. A rough sketch of the velocity field is shown in the right panel of Figure 3. The radial component of Leo's infall along the line of sight from the Local Group to Leo 1 is + 326 ± 37 km S^{-1}. in addition to this, there is of necessity a component of the Local Group infall into Virgo projected along the line of sight to Leo. in this instance the component is -301 ± 37 km s^{-1}. Wc note in passing that these two terms arc almost equal in magnitude but opposite in sign, therefore largely canceling each other in the final determination of the pure expansion velocity of Leo. Removing the infall components from the observed recession velocity, the unperturbed expansion velocity of the Leo 1 Group in this model is then +842 --326 -1 301 = -1817370 km S-]. The Hubble constant derived directly from the velocity field at the 11.2 Mpc distance of the Leo 1 Group is therefore 733 8 km s^{-1} Mpc^{-1}.

The error on the value of the 11 ubble constant quoted immediatel y above only accommodates the combined uncertainties in distance and velocity to first order; there are in fact couplings of the errors through the scaling relations and projection factors. Because of the

non-linearities of these coupling terms we decided to quantify the errors more rigorously by subjecting the full set of equations to a perturbation analysis. By simultaneously allowing the distances, mean velocities and the flow correction to independently scatter by their quoted errors, 1,000 independent calculations of H_o were made. This analysis gives a Hubble constant of 79 ± 14 km s^{-1} Mpc^{-1}. Although the errors were randomly applied as Gaussians with zero mean the derived value of the Hubble constant is larger (by 6 km s^{-1} Mpc^{-1}) than the previous calculation because of a skew (1 .7) in the histogram of Hubble constants (see Fig *) introduced by the non-linear coupling of projection factors. Determining the median value of the Hubble constant and deriving errors from the histogram of simulations we finally derive the following: $H_o(Leo)$ = 76[-{ 9, -- 6}$_{.50}$ [+13, - 9]$_{.68}$[+ 42, – 15].9s, where the quoted errors are 50, 68 and 98% confidence intervals, each reflecting the skew in the probability distribution function.

This same model, obviously, yields an estimate of the Hubble constant directly through Virgo; that value is $H_o = 87 \pm 20$ km s^{-1} Mpc^{-1}. Although this value is consistent, to within the quoted errors, with the Leo Group solution, we can go one step further and demand that the two values agree exactly by solving for the Local Group infall velocity that provides equality. Returning to the error propagation program, but this time allowing the Virgocentric infall to be a free parameter we find that the Hubble constant determined at Virgo and Leo can be brought into coincidence ($H_o = 76$ km s^{-1} Mpc^{-1}) for a Local Group infall velocity of only +135 km s^{-1}.

The foregoing calculations all assume that there are no additional perturbations to the Local flow model outside of the Virgo infall, and that there are no transverse peculiar motions of either the Leo or the Local Group. Moving to larger redshift-distances would alleviate the effects of additional random motions which are not easily measured independently. We can now proceed to estimate the Hubble constant using several different approaches to carry

us into the far-field Hubble flow. First, we calibrate independently, the surface brightness fluctuation] (SBF) method, planetary nebula luminosity function (PNLF) and then the D_n - σ relations. Finally, we use our new distance to the Leo 1 group to step out to the Virgo and Coma clusters.

7.2 Calibration of Secondary Distance Indicators

7.2.1 Surface Brightness Fluctuations

This method is primarily applied to giant elliptical galaxies. It basically measures the second moment of the luminosity function, which is a calibrated function of the (V - *I*) color (Tonry 1991, Jacoby *et al.* 1992). Application of the SBF method to nearby clusters shows that it has a small intrinsic dispersion of ± 0.08 to ± 0.15 mag in the *I* – band (Tonry 1991). However, the major shortcoming of the SBF method is that there is only one Local calibrator, the M31 bulge. Recent discovery of Cepheid variables in M81 (Freedman *et al.* 1994), has supplemented the sample of calibrators, but again, it is the bulge of M81 that is applied in the SBF calibration. It is uncertain at present whether a systematic difference exists between this calibrator and the target galaxies which are mostly giant elliptical galaxies. The TRGB distance to NGC 3379 presents the first step towards resolving this problem, by significantly increasing the number of calibrators and providing a first direct distance to a calibrating giant elliptical galaxy.

The mean fluctuation magnitude is expressed by

$$\bar{M}_I = C + 3(V - I)_{\rm obs} \qquad (2)$$

where C is the zero point, for which Tonry (1991) derives $C = -4.84$ mag. The distance modulus is then written as:

$$(m - M)_{\rm SBF} = \bar{I}_{\rm obs} - C - 3(V - I)_{\rm obs} + 0.80A_B, \qquad (3)$$

where A_B is the extinction in B-band.

Here, we rederive the zero point of the SBF method using the new direct distance to NGC 3379. We assume that the distance to M31 is 770 kpc whit}) corresponds to the distance II1OC]U]US of 24.43 mag (Freedman & Madore 1 990). All the necessary data were taken from 'J'able 2 in Ciardullo, Jacoby & Tonry (1 993: CJT). The zero point determined by using only NGC 3379 is --5.26 msg. If we use all three galaxies - M31, M81 and NGC 3379 we obtain --5.05 msg. We will discuss the implications of these zero points later in this section. We now continue with the calibration of another secondary distance indicator, the planetary nebula luminosity function.

7.2.2 Planetary Nebula Luminosity Function

The [0111] λ5007 luminosity function of faint planetary nebulae follows an exponential law, but at the bright end, the function apparently shows a sharp turnover. The absolute magnitude of this truncation point has been shown to be insensitive to the age and metallicity of the parent stellar population, Thus, the PNLF method is technically applicable to all morphological types of galaxies. However, the app lication of this method has so far been restricted to elliptical galaxies since for late type spirals and irregular galaxies, the total number of HII regions far exceeds that of bright planetary nebulae, making it difficult to distinguish the two, at least with the ground- based observations. Again, one of the major sources of uncertainty in the PNLF method is its absolute calibration]); it relies solely on the planetary nebulae observations in the M31 bulge.

The distance modulus determined by the PNLF method is expressed by:

$$(m - M)_{\rm PNLF} = (m^* - M^*) - 0.85A_B \qquad (4)$$

where m^* and M^* are observed and absolute turnoff magnitude respectively. Again, we adopt the h431 distance of 770 kpc. Ciardullo *et* al. (1 989) obtained m* = 20.17 mag for

the M31 bulge. Substituting this value into equation (4), we get $M^* = -4.52$. Using only the NGC 3379 data, we obtain $M^* = -4.81$. Note that there are more calibration galaxies available now as more Cepheid distances are measured. However, exercise presented here applies only these galaxies published to date.

We now discuss the implications of these newly derived zero points of PNLF and SBF methods.

7.2.3 *Comparison of SBF and PNLF Distances*

CJT reviewed the results of the two methods and analyzed the external and internal errors. They found that the PNLF distances were systematically larger than the SBF distances by 0.13 ± 0.05 mag, but they concluded that this offset was fully consistent with the uncertainties in the calibration.

We have re-calculated the SBF and PNLF distance moduli for eleven galaxies in the Leo I group, Virgo and Fornax clusters and four Coma-cluster galaxies, which were taken from Table 3 of CJT. First, we calculated the two distance moduli using the mean zero point of three calibrators, M31, M81 and NGC 3379. Then the distances were determined by using one calibrator at a time. For each set of zero points, we tabulate the SBF distance modulus, PNLF distance modulus and their difference. Using the M31 bulge only, we get a mean difference of -0.17 ± 0.05 mag, which is consistent with the value determined by CJT. However, we find that if we use NGC 3379 as a sole calibrator, the mean difference is reduced to $+0.03 \pm 0.05$ mag. If we use three calibrators (M31, M81 and NGC 3379), the mean difference becomes $+0.08 \pm 0.05$ mag. The addition of NGC 3379 as a calibrator indeed shifts the zero point in the direction of better consistency between the two methods. Furthermore, it is encouraging that the application of NGC 3379 as a sole calibrator leads to the most consistent result between two methods, perhaps because, of three calibrators,

this galaxy is the only giant elliptical galaxy, the same morphological type as target galaxies for which these distance indicators are applied.

7.2.4 D_n - σ Relation

This distance estimator, developed by Dressler *et al.* (1987), correlates the velocity dispersion of elliptical galaxies with a photometric parameter D_n, which is the diameter at which the integrated surface brightness attains some defined value. The basic idea is that for a given galaxy, D_n is inversely proportional to the distance. This works because the surface brightness is independent of distance, (after correcting for K-dimming and cosmological effects). In large surveys of elliptical galaxies, the D_n - σ relation was primarily used to measure the relative distances between clusters of galaxies, thus the lack of its zero point calibration was not so critical. There have been, however, several attempts at calibrating this relation, including Dressler (1987) where he used bulges of the spiral galaxies M31 and M81. Although the correlation may apply to spiral bulges, we must recall that the bulges have large rotational velocities in addition to the random motions measured by σ. Thus the extension of D_n - σ to these objects assumes that all spiral bulges of a given luminosity have the same ratio of rotational velocity to velocity dispersion. Pierce (1989) later calibrated the D_n - σ - Y relation using two galaxies, NGC 3377 and NGC 3379, in the Leo I group as calibrators, assuming the distance of 10.0 ± 1.0 Mpc obtained from the PNLF method (Ciardullo, Jacoby & Ford 1989) calibrated by Cepheids in M31 (Freedman & Madore 1990). However, as we know, the PNLF method itself has an uncertain zero point calibration because of the small number of calibrators. We therefore recalibrate the D_n - σ relation using the new TRGB distance to NGC 3379.

The D_n -- σ relation is written as:

$$\log R_e = 1.20 \log \sigma - \log D_n + \log\left(1 + \frac{7}{4} z\right) + C \qquad (5)$$

where R is the distance to the target galaxy, and σ is its velocity dispersion. The third term on the right-hand side represents the cosmological correction (Lynden-Bell *et al.* 1988). The $D_n - \sigma$ distance R_c is related to the true distance R via a Malmquist correction relation:

$$R = R_c \exp[3.5(0.21)^2/A^2] \qquad (6)$$

where *0.21* is the dispersion in the $D_n - \sigma$ relation (in units of log D_n) and N is the number of galaxies in a group. For the Leo 1 group, there are two galaxies with $D_n - \sigma$ measurements, NGC 3377 and NGC 3379. Substituting log D_n = 1.24 and log σ = 2.303 for NGC 3379 (Faber *et al.* 1989), we obtain the zero point of C . 5.50. This result will be applied below to estimate the value of Hubble constant.

7.3 Virgo - Coma distance

One approach which circumvents uncertainties in the Virgo velocity due to peculiar motions, is to determine H_0 at the distance of the Coma cluster, (even via Virgo), using the knowledge of the *relative* distances between Leo, Virgo and Coma. These distance ratios are well determined from various secondary-distance indicators such as the SBF, PNLF and D_n - 0 (*c.f.,* de Vaucouleurs 1993).

We proceed as follows: First, the distance ratio of the Virgo cluster and Leo Group is obtained by calculating a mean value of distances obtained by SBF, PNLF and D_n - σ relations using the zero points derived in the above sections. For the PNLF method, observations for three galaxies in Leo 1 and five galaxies in Virgo are available. For SBF, three galaxies in the Leo 1 group have observations and twelve galaxies in Virgo have fluctuation measurements (Tonry, Ajhar & Luppino 1990). All the necessary data for D_n - 0 are presented in Faber *et al.* (1989); for Leo and Virgo, two and sixteen galaxies, respectively, are available. The results are shown in Table 3. The three methods, SBF, PNLF and D_n - 0, respectively give μ(Virgo - Leo 1) = 0.96 ± 0.17, 0.84 ± 0.14 and 1.03 ± 0.16 mag.

Next, wc step from Virgo to the Coma cluster. Unfortunately, there are presently no SBF or PNLF distances to Con-Is; so wc must rely totally on the D_n - σ relation. The difference in distance moduli between Coma and Virgo is μ(Coma)- μ(Virgo)= 3.71 ± 0.10 mag (de Vaucouleurs 1993). Recently, however, it was reported that the Coma cluster is likely to consist of subclusters: the main cluster centered 011 NGC 4374 at cz = +6,853 km s" and a subcluster centered on NGC 4839 at cz = + 7,339 km S--1 (Colless & Dunn 1995). This suggests that distances to Coma obtained by various methods could be affected by a systematic error, if those samples included a substantial number of galaxies in the subcluster region around NGC 4839. Wc re analyzed the D_n - σ data of Faber *et al.* (1 989: F89) in order to inspect if the subclustering affects the measurement of Coma distance significantly. The Coma data in F89 is comprised of 33 elliptical galaxies, 27 of which are located within the main cluster defined by Colless & Dunn. The mean distance modulus of all 33 galaxies is 34.88 mag, while that of central 27 galaxies is 34.91 mag. Furthermore, it is noted that 3 galaxies in the main cluster have D_n - σ distances larger than + 12,000 km s^{-1}. If these galaxies are excluded from the sample, then the remaining 24 galaxies give the mean velocity of +7,195 km s-'. Although the three supposedly 'background' galaxies have significantly large distances, compared to the mean, given that their redshifts do coincide with that of the Coma cluster, they arc probably dynamically associated with the main cluster. The D_n – σ distance modulus of Virgo determined by using equation (5) is 31.21 mag. The difference in distance moduli of the two clusters is then 3.70 ±0.13 msg. The SBF, PNLF and D_n -- σ distan ce modu li of Coma are therefore μ_{Leo} -1 $\delta\mu_{Virgo-Leo}$ + $\delta\mu_{Coma\ -\ Virgo}$ · 34.95 ± *0.26, 34.83* ± *0.24* and 35.06 ± 0.25 mag, respectively. They correspond to linear distances of 983-13, 935.11 and 103 ± 13 Mpc. The radial velocity of the main Coma cluster is +6,853 ± 100 km s"'. As summarized in 'J'able 1, the values of Hubble constant derived by the three methods are then 70 ± 9, 74 ± 9 and 67 ± 8 km s1 Mpc^{-1}.

7.4 Leo I - Coma Relative Distance

Yet another approach is to step directly from the Leo I group to Coma, decreasing the number of steps. Examining D_n -- σ distances to the Leo 1 Group and Coma in F89, the direct distance ratio is μ(Coma)$-\mu$(Leo 1) $= -4.73 \pm 0.13$ mag, which is well within the error of the value we obtained in the previous section. This puts the Coma cluster at $\mu = -35.02 \pm 0.19$ mag. The error in this case (stepping directly from Leo I to Coma) is smaller as expected, but not significantly. The Hubble constant determined by way of stepping directly out to the Coma cluster from Leo 1 is 68 ± 7 km s^{-1} Mpc^{-1}.

This second route of measuring H_o is more accurate, given that fewer parameters enter into this exercise. Still, the Hubble constant derived by the four separate methods agree with each other extremely well. Taking their mean value, we find $H_o = 703$ 10 km s^{-1} Mpc^{-1}. As a point of comparison we note that Tanvir *et al.* (1995) obtained $H_o = 69 \pm 8$ km s^{-1} Mpc^{-1} using the Cepheid observations of NGC 3368 in the Leo 1 group.

In Table 2, we list all systematic and random errors. The dominant terms are the random errors in measuring the position of the TRGB and in the ratio of distances to the clusters. Also systematic errors in the calibration of the TRGB method and those in the distances to Galactic globular clusters are significant. We especially focus on the uncertainties in the TRGB calibration arising from its uncertain zero point in the higher metallicity range. Even if the metallicity of the NGC 3379 halo turns out to be much higher than the value adopted here and the blanketing effect becomes non-negligent, we note that this would make the tip magnitude fainter. Consequently, the distance modulus of NGC 3379 would decrease, which in turn would raise the value of H_o. Therefore, the Hubble constant determined in this paper represents a lower limit.

8 Discussion and Conclusions

Individual stars at the tip of the Population II red giant branch have been detected in the giant elliptical galaxy NGC 3379. Identifying the abrupt discontinuity of the apparent luminosity function at $I = 26.29 \pm 0.10$ mag with the TRGB at $M_I = -4.0$ mag gives a distance of 11.4 ± 0.8 Mpc to NGC 3379. Extrapolating the Leo 1 distance to Coma using a well-determined distance ratio of two groups from $D_n - \sigma$ studies, we measure the H_o at the distance of Coma to be 704.11 km s^{-1} Mpc^{-1}. This is the most distant application of the TRGB method to date, aud is fully consistent with the Cepheid-based distance to this group as also recently determined by 11 S'1'. In Figure 4, the comparison of distances derived by Cepheid PL relation and TRGB method is shown, further demonstrating the accuracy of the TRGB method as a distance indicator.

We must not, however, be overly optimistic. At very high metallicities the calibration of the TRGB is not yet w c]] established; but an effort to obtain a more precise calibration is currently being undertaken by us. Also, even though we are fortunate in the case of NGC 3379 to have encountered a relatively small population of intermediate-age AGB stars, this could pose a problem in some galaxies when measuring the TRGB position using the I-band luminosity function. Nonetheless this paper gives another solid example of how powerful and promising the TRGB method can be as a distance indicator and demonstrates its versatile applicability to various types of galaxies.

We thank Dr. Peter Stetson for providing us with WFPC2 vignetting masks. This paper made usc of the NASA/IPAC Extragalactic Database (NED) which is operated by the Jet Propulsion laboratory, California Institute of Technology, under contract with the National Aeronautics and Space Administration. BFM was supp orted in part by NED and by JPL. WLF was supported in part by NSF grant AST 91-16496.

REFERENCES

Bica, E., Barbuy, B. & Ortolani, S., 1991, ApJ, 382, 1,15

Burstein, D. & Heiles, C., 1984, ApJS, 54, 33

Ciardullo, R., Jacoby, G. H. & Ford, H. C., 1989, ApJ, 344, 715

Couture, J., Harris, W. E. & Allright, J. W. B., 1990, ApJ, 73, 671

Da Costa, G. S. & Armandroff, T. E., 1990, AJ, 100, 162

de Vaucouleurs, G., 1975, "Stars and Stellar System" Vol. 9, University of Chicago Press, ed. A. Sandage, M. Sandage & J. Kristian

de Vaucouleurs, G., 1993, ApJ, 415, 10

Dressler, A., Lynden-Bell, 1)., Burstein, 1)., Davies, 11. 1,., Faber, S. h4., Terlevich, R. J. & Wegner, G., 1987, ApJ, 313, 42

Faber, S. M., Wegner, G., Burstein, 1)., Davies, R. L., Dressler, A., Lynden-Bell, 1). & Terlevich, R. J., 1989, 69, 763

Freedman, W. L. & Madore, B. F., 1990, ApJ, 365, 186

Freedman, W. 1,. & Madore, B. F., 1996, ASI' Review Series, ed. V. Trimble, "Clusters, Lensing and the Future of the Universe').

Goudfrooij, 1'., Hansen, L., Jorgensen, H. E., Norgaard-Nielsen, 11. U., de Jong, '1'. & van den Hoek, 1,. 11., 1994, A&AS, 104, 179

Green, E. M., Demarque, 1'. & King, C. R., 1987, The Revised Yale Isochrones and Luminosity Functions (New Haven: Yale Univ. Obs

Han, h4. & Mould, J., IWO, ApJ, 360, 448

Hutterer, Sasselov & Schechter 1995, AJ, Preprint

Lee, M. G., Freedman, W. L. & Madore, B. F., 1993, ApJ, 417, 553

Madore, B. F. & Freedman, W. L., 1995, AJ, 109, 1645

Madore, B. F., Freedman, W. L. & Lee, M. G., 1993, AJ, 104, 2243

Mould, J. & Kristian, J., 1986, ApJ, 305, 591

Ortiz, P., 1990, PhD Thesis, University of Toronto

Pahre, M. A. & Mould, J. R., 1994, ApJ, 433, 567

Pierce, M. J., 1989, ApJ, 344, 1,57

Sakai, S., Madore, B. F. & Freedman, W. L., 1995, ApJ, in press

Stetson, P. B., 1987, PASP, 99, 191

Stetson, P. B., 1994, PASP, 106, 250

Stetson, P. B., 1995, Private Communication

Tanvir, N. R., Shanks, T., Ferguson, H. C. & Robinson, D. R. T., 1995, Nature, 377, 27

Tonry, J. L., Ajhar, E. A. & Luppino, G. A., IWO, AJ, 100, 1416

Figure Captions

Figure 1: luminosity functions and their corresponding edge detection response functions. A line representing a slope of 0.6 dex/mag is overplotted on the logarithmic luminosity function. The response function corresponding to the logarithmic luminosity function) was weighted by square root of the luminosity function.

Figure 2: Average edge detection response histogram Of 500 iterations (see text for details). All 'signals' below $I = 26.0$ mag are very likely noise, making the TRGB detection more prominent.

Figure 3: A rough sketch showing the geometry of Local Group, Leo I Group and Virgo cluster used in our simple Virgocentric infall model.

Figure 4: Comparison of distances obtained by the TRGB method and Cepheid PL relation.

Table 1
Hubble Constant

Method	$\delta\mu$ (Virgo - Leo)	$\delta\mu$ (Coma - Leo)[a]	μ (Coma)'	$H_o \pm$ random $\pm$ systematic
(1) Stepping from Leo I to *Coma* via Virgo				
SBF	0.96 ± 0.17	4.66 ± 0.21	34.95 ± 0.22	$70 \pm 8 \pm 5$
PNLF	0.84 ± 0.14	$4..54 \pm 0.19$	34.83 ± 0.22	$74 \pm 8 \pm 6$
$D_n - \sigma$	1.03 ± 0.16	4.73 ± 0.21	35.06 ± 0.23	$67 \pm 8 \pm 5$
(2) Stepping from Leo I to Coma directly:		4.73 ± 0.13	$3.5.02 \pm 0.17$	$68 \pm 6 \pm 5$
(3) Virgocentric infall model fro Leo I:				$73 \pm 8 \pm 5$

[a] Adopted $\delta\mu$(Coma - Virgo) = 3.70 ± 0.13 from $D_n - \sigma$.
[b] Only the random errors are included here. The systematic error is +0.15 msg.

Table 2

Error Budget

Source	Error (mag)
Random Errors:	
Galactic. extinction	± 0.02
Tip Measurement	±0.10
Leo Coma Distance Ratio (D_n -- σ)[a]	±0.13
Velocity of Coma (100 km s])	:10.02
Total Random Uncertainty	±0.17
Systematic Errors:	
RR Lyrae Distance Scale Zero Point	± 0.10
TRGB Calibration (Metallicity)	:10.10
Photometric zero point (WFPC 2)	±0.04

[a] Wc are only snowing the error corresponding to the case (2) in 'J'able 1 as an example here.

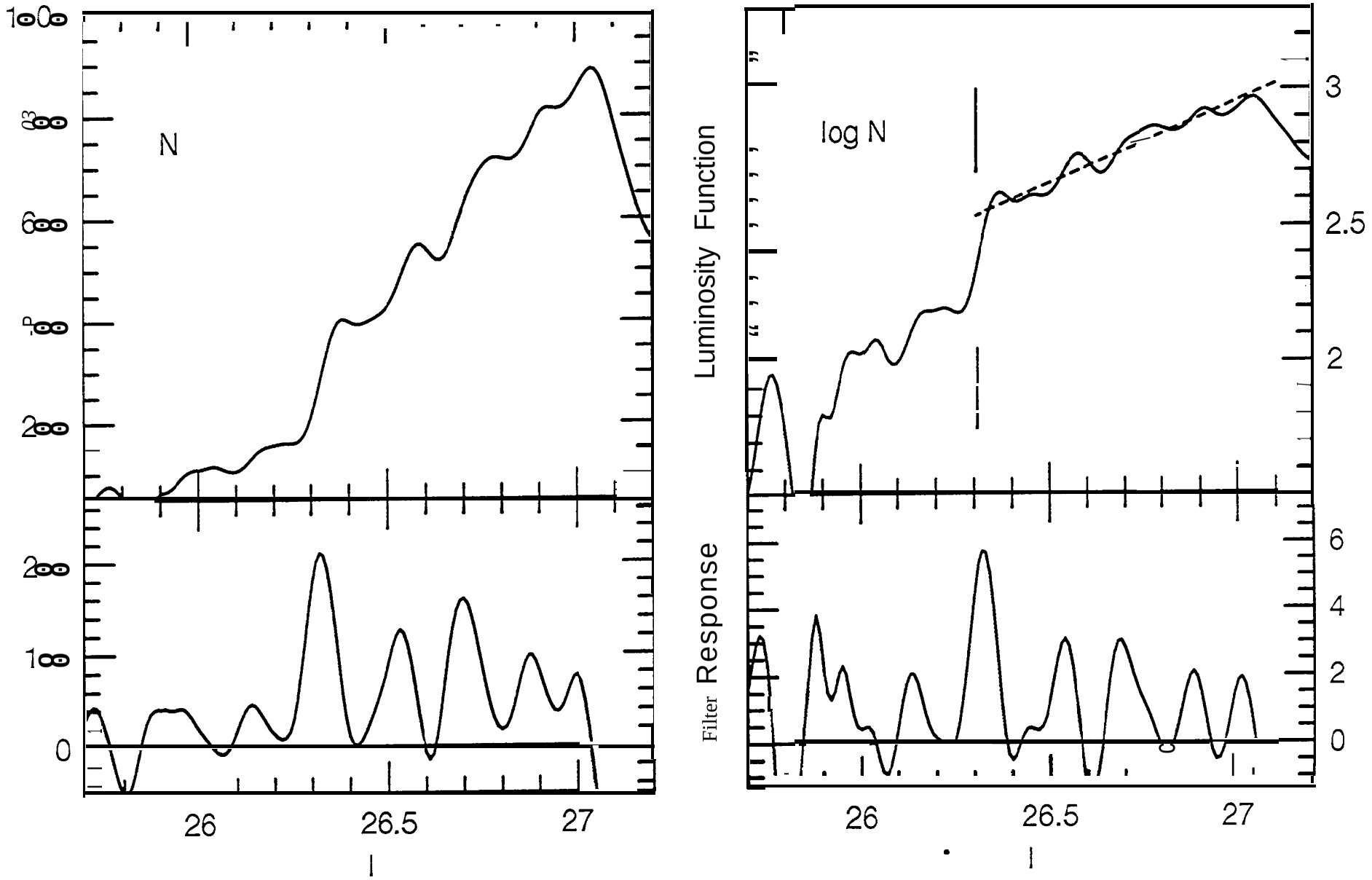
N
log N
Luminosity Function
Filter Response
26
26.5
27
3
2.5
2
6
4
2
0

FIGURE 1

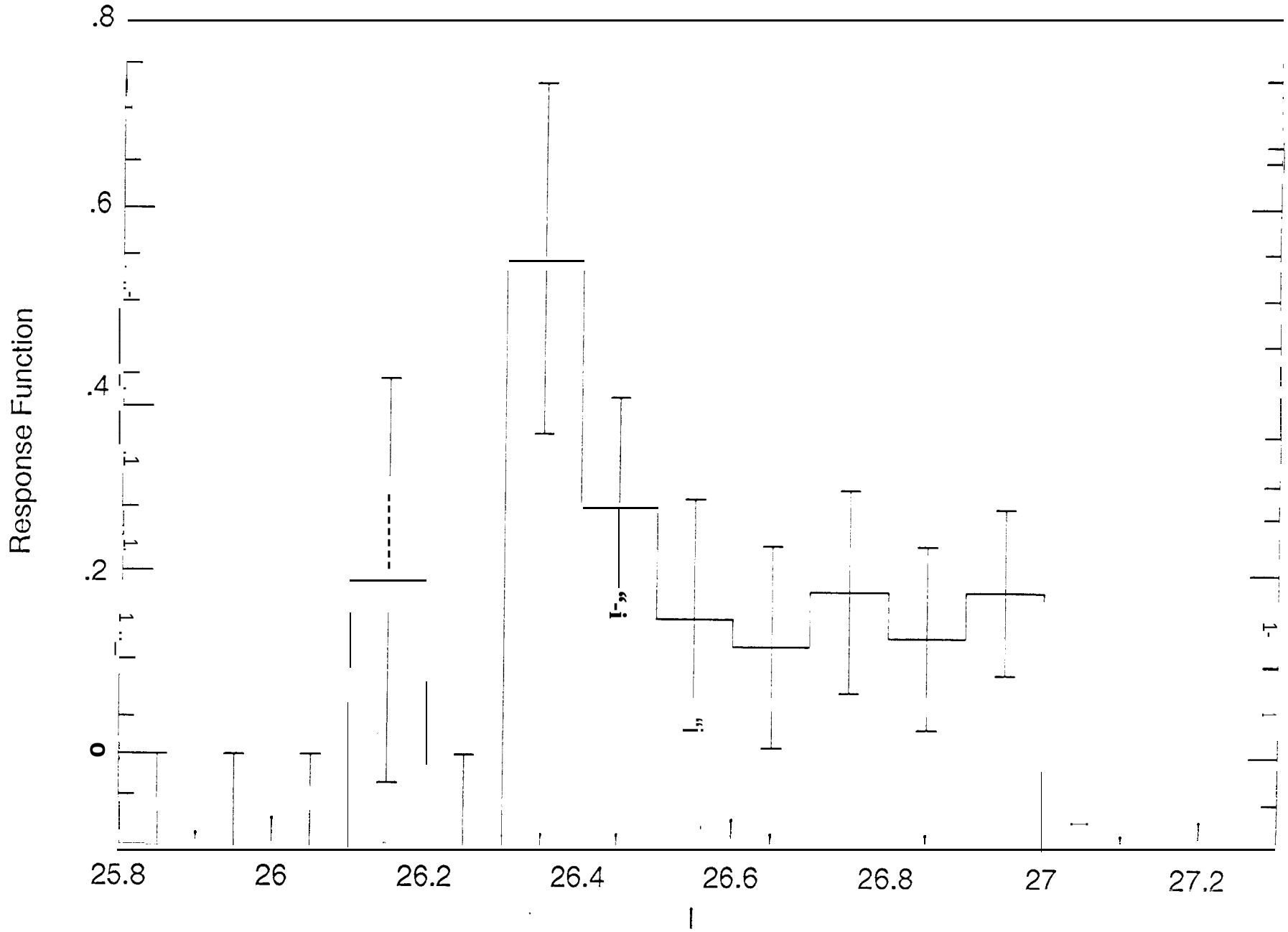

FIGURE2

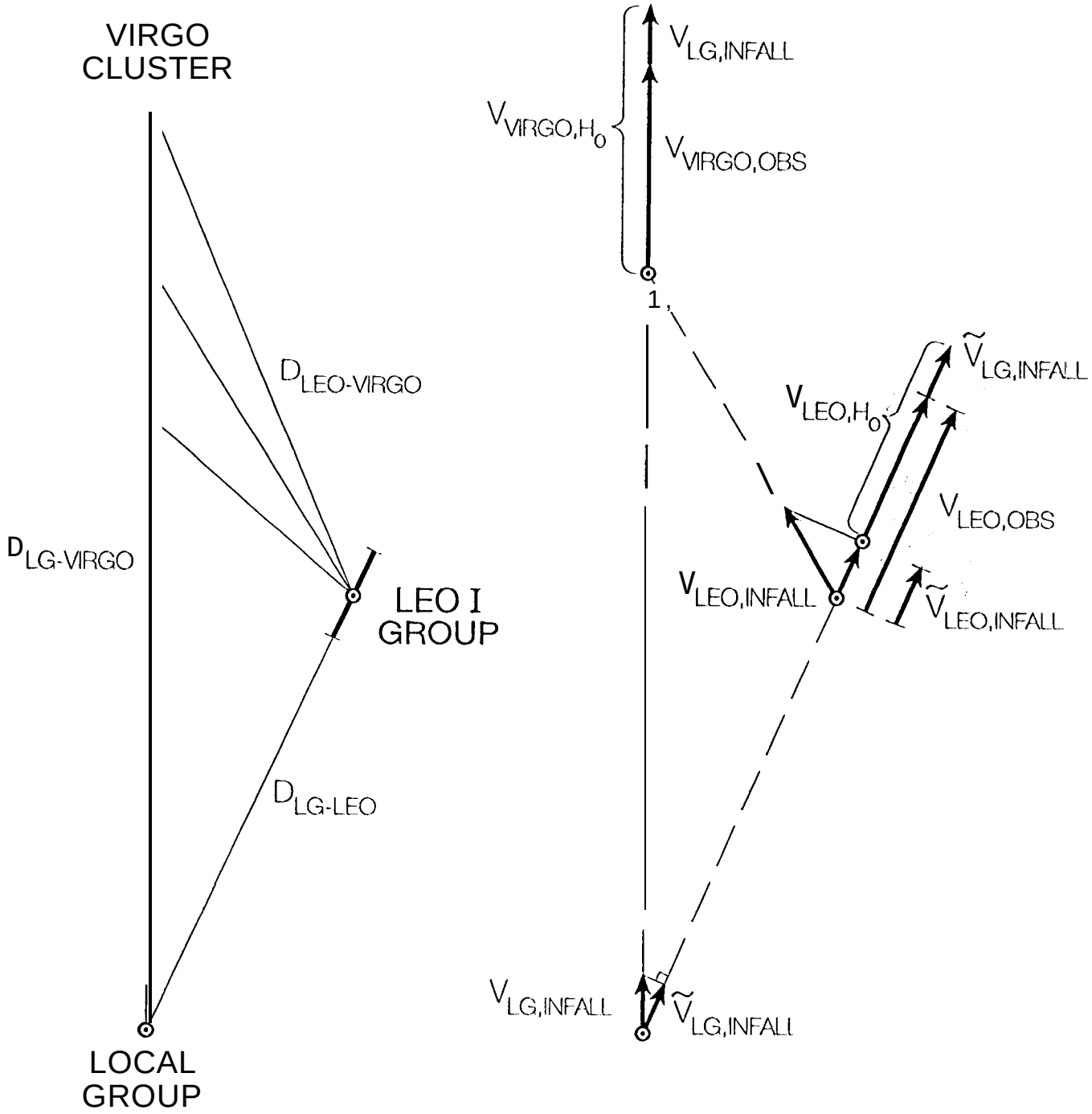
VIRGO
CLUSTER
$D_{LEO-VIRGO}$
$D_{LG-VIRGO}$
LEO I
GROUP
D_{LG-LEO}
LOCAL
GROUP
$V_{LG,INFALL}$
V_{VIRGO,H_0}
$V_{VIRGO,OBS}$
1
$\tilde{V}_{LG,INFALL}$
V_{LEO,H_0}
$V_{LEO,OBS}$
$V_{LEO,INFALL}$
$\tilde{V}_{LEO,INFALL}$
$V_{LG,INFALL}$
$\tilde{V}_{LG,INFALL}$

FIGURE 4

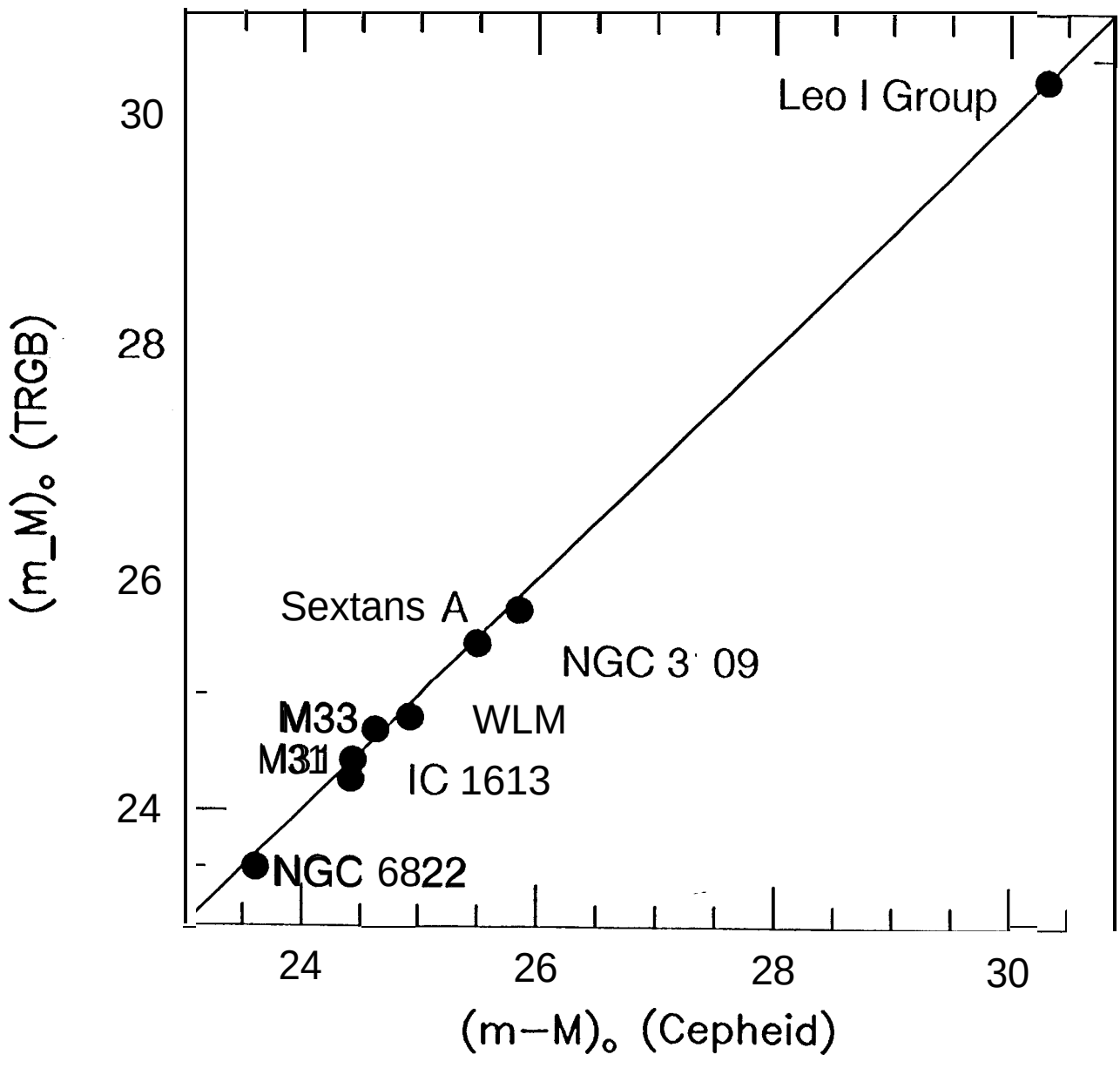
Leo I Group
Sextans A
NGC 3 09
M33
WLM
M31
IC 1613
NGC 6822
30
28
26
24
24
26
28
30
(m_M)₀ (TRGB)
(m−M)₀ (Cepheid)